Inhibition of low-carbon steel corrosion by derivatives of 4,5,6,7-tetrahydro-[1,2,4]triazolo[1,5-*a*]pyrimidin-7-ol

D.V. Lyapun, D.S. Shevtsov,* A.A. Kruzhilin, O.A. Kozaderov, I.V. Avetisyan, D.A. Machnev, I.D. Zartsyn and Kh.S. Shikhaliev

Voronezh State University, Universitetskaya pl. 1, 394018 Voronezh, Russian Federation
**E-mail: shevtsov@chem.vsu.ru*

Abstract

The ability of four compounds of 4,5,6,7-tetrahydro-[1,2,4]triazolo[1,5-*a*]pyrimidin-7-ol class with different alkyl radical lengths to reduce the corrosion rate of low-carbon steel in a solution of 24% HCl has been established. Using a complex of electrochemical research methods (potentiodynamic measurements, impedance spectroscopy) and quantum chemical calculations, the inhibitory effect of the compounds under consideration was revealed. Analysis of the polarization curves showed that all the studied compounds decrease both the anodic and cathodic current density, behaving as the inhibitors with a mixed protective effect. The introduction of the additives causes an increase in the radius of the semicircles on the Nyquist diagrams relative to the control experiment without changing the shape of the hodograph. According to the results of potentiodynamic measurements and electrochemical impedance spectroscopy, a proportional increase in the polarization resistance of the electrochemical reaction was observed. The degree of protection is similar for the investigated additives at the same concentration (C_{inh}), and it practically does not change in the series of substituents from R–H to R–C_3H_7. With an increase of C_{inh} from 1.0 to 2.0 g·dm^{-3}, the inhibition efficiency increases. The results of experimental electrochemical research and quantum chemical studies correlate with each other. According to electrochemical measurements, the highest degree of protection (up to 94%) was obtained for 5-phenyl-4,5,6,7-tetrahydro-[1,2,4]triazolo[1,5-*a*]pyrimidin-7-ol at C_{inh}=2.0 g·dm^{-3}. The proposed corrosion inhibitors can be used at oil and gas production facilities to reduce the rate of corrosion when using acid solutions in the bottom-hole zone of wells and building structures, including those based on reinforced concrete.

Received: November 15, 2023. Published: December 6, 2023 doi: 10.17675/2305-6894-2023-12-4-43

Keywords: *corrosion, low-carbon steel, inhibitors, derivatives of 4,5,6,7-tetrahydro-[1,2,4]triazolo[1,5-a]pyrimidin-7-ol.*

Introduction

In the oil industry, acid treatments are usually used to intensify oil and gas recovery of wells in order to create artificial channels in carbonate formations and increase their permeability. This is achieved by dissolving clay and other materials that can clog pores in the bottomhole area of the well. For this purpose, acetic, hydrochloric or a combination of hydrofluoric and hydrochloric acids are most often used [1–3]. Such solutions cause accelerated corrosion

inside casing pipes and columns of flexible tubing, and also contribute to the corrosion degradation of reinforced concrete structures of the oil and gas complex as a whole [4]. To reduce the negative effect, so-called "inhibited acids" are used, which are formed by adding specific corrosion inhibitors to the initial acid solution [5, 6]. Despite the fact that today there are a number of organic corrosion inhibitors that can be used to solve this problem [7], the search for new organic compounds that are potentially more effective both in terms of their cost, cost-effectiveness, as well as biodegradability and harmlessness, and in terms of their anticorrosive activity remains an urgent task.

Previously, an unexpected inhibitory effect of mixtures of 3-alkyl-5-amino-1*H*-1,2,4-triazoles and cinnamic aldehyde was found [8] against corrosion of steel in solutions of 24% hydrochloric acid. A comprehensive study of the composition of these mixtures showed that they contain a new class of previously unexplored inhibitors of acid corrosion of steel – 4,5,6,7-tetrahydro-[1,2,4]triazolo[1,5-*a*]pyrimidin-7-ols. Probably, the high protective effect of these substances on steel in HCl solutions is due to the presence of a triazolopyrimidine matrix in their structure. The matter is significant protective properties under these conditions were absent in the initial short-chain 3-alkyl-5-amino-1*H*-1,2,4-triazoles, from which the compounds studied in this article were obtained [9]. In turn, cinnamon aldehyde in its pure form also did not show degrees of protection of more than 50–60%. At the same time, earlier in [10] derivatives of [1,2,4]triazolo[1,5-*a*]pyrimidine, also obtained on the basis of 3-alkyl-5-amino-1*H*-1,2,4-triazoles, showed significant anticorrosive activity (degree of protection 70–90%) against copper chloride corrosion.

In this regard, the purpose of this work was a comprehensive study of the anticorrosive properties of four new, previously undescribed, compounds of 4,5,6,7-tetrahydro-[1,2,4]triazolo[1,5-*a*]pyrimidin-7-ols class with respect to corrosion of low-carbon steel in acid chloride solution.

Experimental

A series of 4,5,6,7-tetrahydro-[1,2,4]triazolo[1,5-*a*]pyrimidin-7-ols differing in the presence and length of a hydrocarbon radical has been studied as potential corrosion inhibitors of low-carbon steel (Table 1).

Table 1. Designations, names and structural formulas of the studied inhibitors.

Symbol	Name	Formula
a	5-Phenyl-4,5,6,7-tetrahydro-[1,2,4]triazolo[1,5-*a*]pyrimidin-7-ol	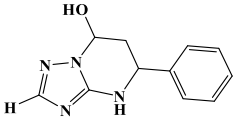
b	2-Methyl-5-phenyl-4,5,6,7-tetrahydro-[1,2,4]triazolo[1,5-*a*]pyrimidin-7-ol	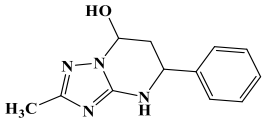

Symbol	Name	Formula
c	2-Ethyl-5-phenyl-4,5,6,7-tetrahydro-[1,2,4]triazolo[1,5-*a*]pyrimidin-7-ol	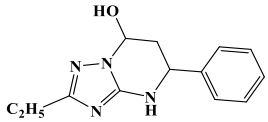
d	2-Propyl-5-phenyl-2-propyl-4,5,6,7-tetrahydro-[1,2,4]triazolo[1,5-*a*]pyrimidin-7-ol	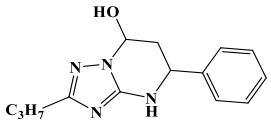

Electrochemical methods were used to evaluate the inhibitory effect. During the measurements, low-carbon steel of the St3 type was used as a working electrode. All surfaces, with the exception of the working one, were reinforced with epoxy resin.

A saturated silver/silver chloride reference electrode (SCE, potential +201 mV relative to the standard hydrogen electrode) was placed in a separate vessel connected to an electrochemical cell by an agar-agar-based electrolytic key filled with a saturated KNO_3 solution. The potentials in the paper are given relative to SCE. The auxiliary electrode was a platinum grid.

Hydrochloric acid (24% by weight) was used as the working solution. Electrochemical measurements were carried out in a three-electrode glass cell with undivided electrode spaces at a temperature of 23±3°C under conditions of natural aeration without additives (control experiment) and with the addition of the studied organic substances.

The working steel electrode was pre-cleaned on K2000 sandpaper, washed with distilled water and degreased with chemically pure isopropyl alcohol. The current density i was calculated by dividing the recorded current strength I by the geometric area of the working electrode (1.0 cm^2).

The corrosion current density (i_{cor}) was determined by the Mansfeld polarization resistance method [11]. After stabilizing a stationary value of the free corrosion potential (E_{cor}) for 30 minutes, the polarization curve was recorded using the IPC-Pro potentiostat in a potentiodynamic mode (potential scan rate was 0.2 $mV \cdot s^{-1}$) in the range from $E_{cor} - 30$ mV to $E_{cor} + 30$ mV.

The ability of the studied substances to reduce the rate of corrosion was estimated by the degree of protection, which was calculated by the formula:

$$Z_i = \frac{i_{cor,0} - i_{cor,inh}}{i_{cor,0}} \cdot 100\%,$$

where $i_{cor,0}$ and $i_{cor,inh}$ are the corrosion current densities in the control experiment (without additive) and in the presence of an inhibitor, respectively.

Electrochemical impedance spectra were recorded using IPC-Pro potentiostat with FRA-2 frequency response analyzer. After stabilizing a stationary E_{cor} value (for 30 minutes), a frequency dependence was recorded in the range from 0.01 Hz to 50 kHz in an open circuit mode. The analysis of the frequency dependence, the selection of an

equivalent circuit and the determination of the nominal values of its components were carried out in the DCS software package. The results were presented in the form of Nyquist diagrams. The inhibition efficiency (η_{inh}) was calculated by the formula:

$$\eta_{inh} = (1 - \frac{R_{p,0}}{R_{p,inh}}) \cdot 100\%,$$

where $R_{p,0}$ and $R_{p,inh}$ – the polarization resistance found according to the data of impedance measurements in the control experiment and in the presence of an inhibitor, respectively.

In order to further interpret and substantiate the found anticorrosive properties of the studied compounds, quantum chemical calculations of their main characteristics were carried out. Optimization of the molecules geometry was carried out within the framework of density functional theory (DFT) using the B3LYP functional with a basis of 6-311+G(d,p) in the Gaussian 09 package. The optimized geometry of the molecules is characterized by the absence of negative oscillation frequencies and, therefore, corresponds to the minimum value on the surface of the potential energy. In addition, in order to find the five lowest electronic excitations, TDDFT (time-dependent density functional theory) calculations were performed for the optimized geometry. The energies of the boundary molecular orbitals (HOMO and LUMO) are used to predict the effectiveness of inhibition effect of molecules. Within the limitation of Koopmans' theorem, they are given by the following formulas:

$$-E_{HOMO} = IP \text{ and } -E_{LUMO} = EA,$$

here *IP* – ionization potential, *EA* – electron affinity. The inhibitory effect was evaluated by comparing the values of chemical hardness

$$\eta = \frac{IP - EA}{2},$$

and softness

$$\sigma = \frac{1}{\eta}.$$

Results and Discussion

Potentiodynamic measurements

The addition of substances ***a***, ***c*** and ***d*** in the concentration range C_{inh}=1.0–2.0 g·dm^{-3} does not change the E_{cor} value (Table 2). For compound ***b***, its displacement in the anodic direction by 20–50 mV was obtained. At the same time, for all cases, a decrease in current density is observed both on the anodic and cathodic sections of the polarization curves relative to the control experiment without additives (Figure 1).

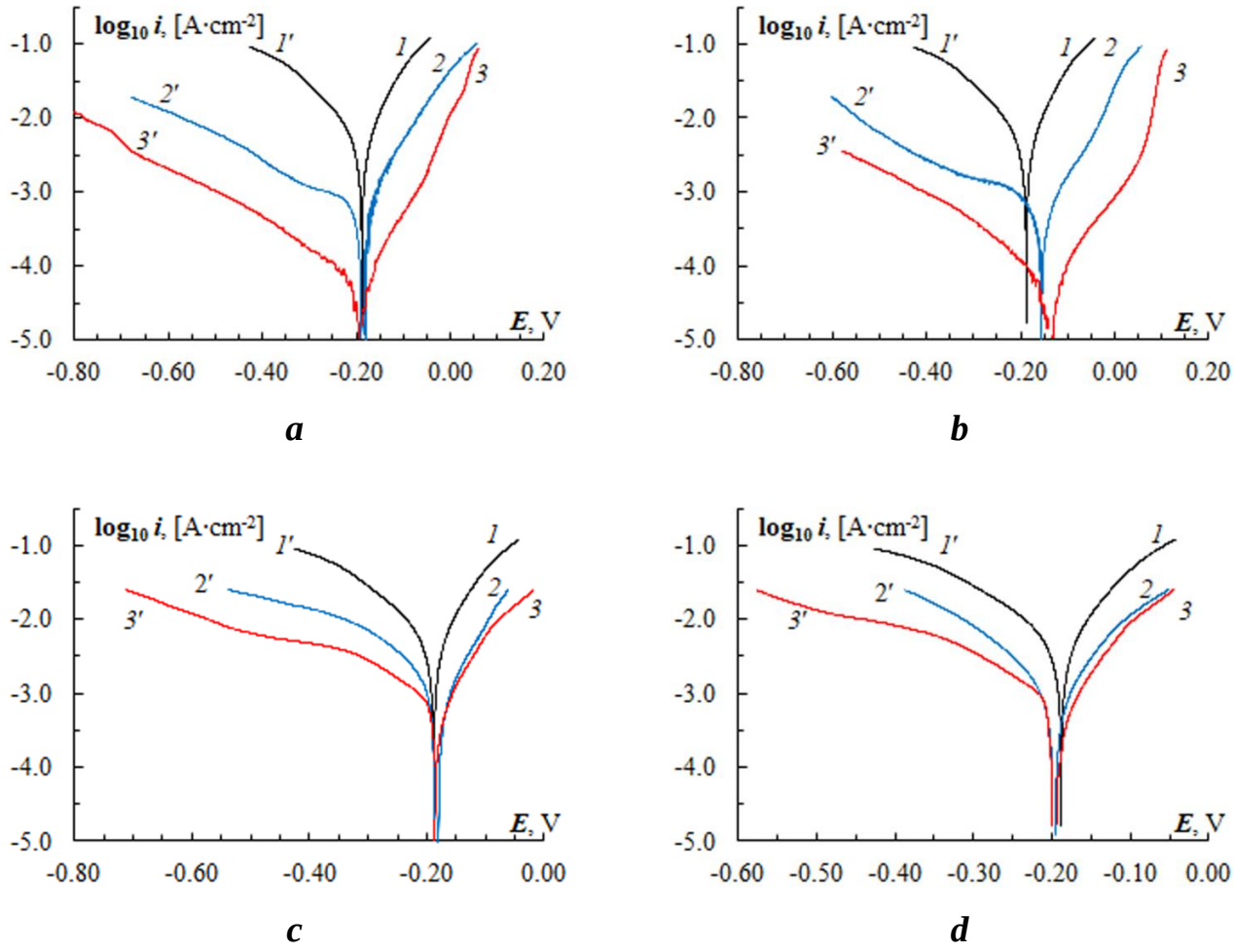

Figure 1. Anodic and cathodic polarization curves of mild steel in 24% HCl without an inhibitor (*1*) and in the presence of 5-phenyl-4,5,6,7-tetrahydro-[1,2,4]triazolo[1,5-*a*]pyrimidin-7-ol (***a***), 2-methyl-5-phenyl-4,5,6,7-tetrahydro-[1,2,4]triazolo[1,5-*a*]pyrimidin-7-ol (***b***), 2-ethyl-5-phenyl-4,5,6,7-tetrahydro-[1,2,4]triazolo[1,5-*a*]pyrimidin-7-ol (***c***) and 2-propyl-5-phenyl-2-propyl-4,5,6,7-tetrahydro-[1,2,4]triazolo[1,5-*a*]pyrimidin-7-ol (***d***) at C_{inh}=1.0 (*2*) and 2.0 g·dm^{-3} (*3*).

Thus, a mixed inhibition mechanism can be assumed, in which the reaction of metal oxidation and reduction of the oxidant (H^+) is affected [12]. At the same time, with an increase in the concentration of the additive, the current density decreases.

The results of calculations of the corrosion rate and degree of protection are consistent with the shape of the polarization curves (Table 2). For all the studied substances at C_{inh}=1.0 g·dm^{-3}, the Z_i values are close (taking into account the determination error) and are in the range 84.9–86.0%. With an increase in the concentration of the additive to C_{inh}=2.0 g·dm^{-3}, the degree of protection increases. The highest values were obtained at the level of 94–95% for compounds ***a*** and ***b***.

Table 2. Kinetic parameters of mild steel corrosion in 24% HCl in the presence of derivatives of 4,5,6,7-tetrahydro-[1,2,4]triazolo[1,5-*a*]pyrimidin-7-ol.

Inhibitor	C_{inh}, g·dm^{-3}	E_{cor}, mV	R_p, kΩ·cm^2	i_{cor}, mA·cm^{-2}	Z_i, %
Blank	–	–191±6	4.2±0.5	6.8±0.3	–
a	1.0	–210±7	25±3	0.99±0.13	85.4
	2.0	–190±5	42±3	0.36±0.06	94.7
b	1.0	–160±9	22±3	1.03±0.19	84.9
	2.0	–135±7	52±4	0.28±0.09	95.9
c	1.0	–191±8	25±3	1.01±0.16	85.1
	2.0	–183±6	39±7	0.49±0.06	92.8
d	1.0	–200±7	23±3	0.95±0.17	86.0
	2.0	–193±6	38±6	0.52±0.09	92.4

Electrochemical impedance spectroscopy

The Nyquist diagrams obtained in the control experiment and in the presence of the studied substances have the same shape, consisting of two distorted semicircles of varying diameter (Figure 2).

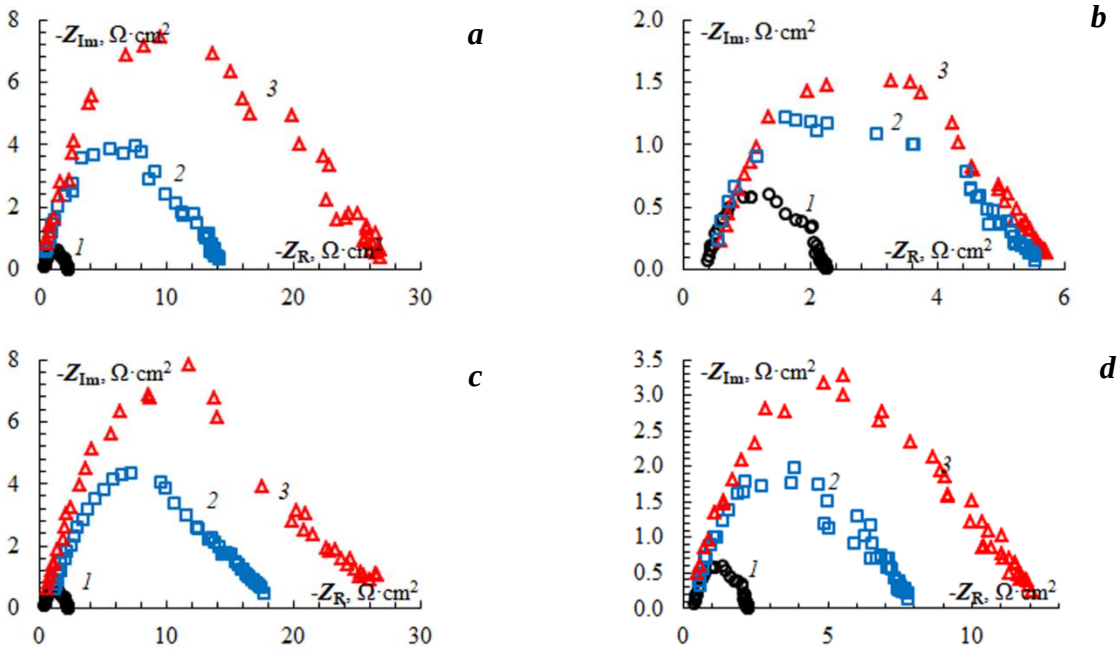

Figure 2. Nyquist diagrams of mild steel in 24% HCl without an inhibitor (*1*) and in the presence of 5-phenyl-4,5,6,7-tetrahydro-[1,2,4]triazolo[1,5-*a*]pyrimidin-7-ol (***a***), 2-methyl-5-phenyl-4,5,6,7-tetrahydro-[1,2,4]triazolo[1,5-*a*]pyrimidin-7-ol (***b***), 2-ethyl-5-phenyl-4,5,6,7-tetrahydro-[1,2,4]triazolo[1,5-*a*]pyrimidin-7-ol (***c***) and 2-propyl-5-phenyl-2-propyl-4,5,6,7-tetrahydro-[1,2,4]triazolo[1,5-*a*]pyrimidin-7-ol (***d***) a at concentrations of 1.0 (*2*) and 2.0 g·dm^{-3} (*3*).

Electrochemical impedance spectroscopy was used to confirm the results of potentiodynamic measurements and to obtain additional information about the mechanism of protective action of the analyzed substances and compositions. When analyzing the results obtained in the presence of organic additives, an equivalent circuit was used, presented in Figure 3 and repeatedly confirmed in similar media [13, 14].

According to the results of calculations (Table 3), the impedance data for compounds ***a***, ***c*** and ***d*** correlate with the results of potentiodynamic measurements. At the same time, the absolute values of η_{inh} are slightly lower compared to Z_i.The lowest inhibition efficiency was found for substance ***b***, and the highest value of η_{inh}=93% was obtained for compound ***a***.

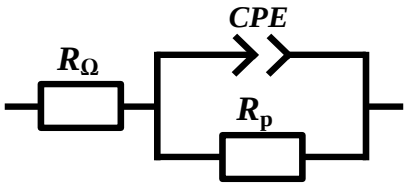

Figure 3. Scheme for describing the experimental results of EIS for the studied inhibitors (R_Ω – ohmic resistance, CPE – constant phase element of the electrochemical reaction, R_p – polarization resistance of the electrochemical reaction).

Table 3. Calculated parameters of equivalent circuit elements of mild steel electrode in 24% HCl in the presence of derivatives of 4,5,6,7-tetrahydro-[1,2,4]triazolo[1,5-*a*]pyrimidin-7-ol.

Inhibitor	C_{inh}, g·dm^{-3}	Equivalent circuit element				η_{inh}, %
		R_Ω, Ω·cm^2	R_p, Ω·cm^2	CPE_T, μF·cm^{-2}	CPE_Φ	
Blank	–	0.23±0.09	1.93±0.03	1.9±0.4	0.75±0.02	–
a	1.0	0.29±0.06	14.3±1.2	0.57±0.18	0.68±0.02	86.4±1.2
	2.0	0.28±0.05	28±2	0.40±0.12	0.69±0.03	93.0±0.6
b	1.0	0.36±0.04	4.8±0.4	1.21±0.17	0.68±0.02	60±3
	2.0	0.39±0.13	5.5±0.4	1.35±0.09	0.61±0.05	65±2
c	1.0	0.36±0.09	15±2	1.05±0.14	0.62±0.02	86±3
	2.0	0.25±0.04	20±3	0.75±0.09	0.63±0.02	90±2
d	1.0	0.21±0.05	7.8±0.4	1.51±0.17	0.63±0.03	75±2
	2.0	0.19±0.06	10.1±0.8	1.41±0.13	0.61±0.07	80±3

CPE_T – capacitance of a "non-ideal" capacitor corresponding to the double electric layer of the real metal/solution interface; CPE_Φ – degree of deviation of the phase angle from its value for an "ideal" capacitor (90°).

Quantum chemical calculations

The calculated values of the energy difference of the highest occupied and lowest unoccupied orbitals, as well as the absolute hardness for all analyzed compounds are close: the difference does not exceed 1.8% (Table 4). This indicates that the ability of the studied 4,5,6,7-tetrahydrotriazolopyrimidinols to adsorption and their inhibitory effect is close in magnitude, which correlates with the results of electrochemical measurements.

Table 4. Calculated energies of E_{HOMO}, E_{LUMO}, HOMO LUMO gaps (*HLG*), ionization potential (*IP*), electron affinity (*EA*), absolute hardness (η) and softness (σ) in eV at B3LYP/6-31G(d,p) level.

Inhibitor	E_{HOMO}, eV	E_{LUMO}, eV	*HLG*, eV	*IP*, eV	*EA*, eV	η, eV	σ, eV^{-1}
a	–6.348	–0.940	5.408	6.348	0.940	2.704	0.370
b	–6.206	–0.898	5.308	6.206	0.898	2.654	0.377
c	–6.203	–0.893	5.311	6.203	0.893	2.655	0.377
d	–6.203	–0.900	5.302	6.203	0.900	2.651	0.377

Conclusion

Based on the results of a electrochemical estimation, the possibility of using bicyclic compounds of the 4,5,6,7-tetrahydro-[1,2,4]triazolo[1,5-*a*]pyrimidin-7-ols class with different alkyl radical lengths at concentrations in the range of 1–2 $g \cdot dm^{-3}$ as corrosion inhibitors of low-carbon steel in acid chloride solutions is shown.

The effectiveness of the application for all studied compounds is close at an equal concentration and increases with an increase in the concentration of the substance in solution. The data of potentiodynamic measurements, electrochemical impedance spectroscopy and quantum chemical calculations correlate with each other.

According to electrochemical measurements, the highest degree of protection (up to 94%) was obtained for 5-phenyl-4,5,6,7-tetrahydro-[1,2,4]triazolo[1,5-*a*]pyrimidin-7-ol a at a concentration of 2.0 $g \cdot dm^{-3}$.

Acknowledgements

The study was supported by the Russian Science Foundation (RSF), project no. 22-23-01144, https://rscf.ru/en/project/22-23-01144/.

References

1. C.N. Fredd and H.S. Fogler, Alternative stimulation fluids and their impact on carbonate acidizing, *SPE J.*, 1998, **3**, no. 1, 34–41. doi: 10.2118/31074-PA
2. B.M. Nasution, A. Yonathan, M. Abdillah and W. Zhen, Pre-Treatment Experimental Study of Organic Acid: An Alternative Means to Overcome Inorganic Scale Build-Up Problem in Deep Well, *SPE Asia Pacific Oil and Gas Conference and Exhibition*, 2021. doi: 10.2118/205693-MS

3. N. Li, F. Chen, J. Yu, P. Han and J. Kang, Pre-acid system for improving the hydraulic fracturing effect in low-permeability tight gas reservoir, *J. Pet. Exp. Prod.*, 2021, **11**, 1761–1780. doi: 10.1007/s13202-021-01129-x
4. D.B. Hammad, N. Shafiq and M.F. Nuruddin, Vectors of defects in reinforced concrete structures in onshore oil and gas process plants, *Adv. Civ. Eng.*, 2018, 3953972. doi: 10.1155/2018/3953972
5. M. Askari, M. Aliofkhazraei, R. Jafari, P. Hamghalam and A. Hajizadeh, Downhole corrosion inhibitors for oil and gas production – a review, *Appl. Surf. Sci. Adv.*, 2021, **6**, no. 6, 100128. doi: 10.1016/j.apsadv.2021.100128
6. V.S. Saji and S.A Umoren, *Corrosion inhibitors in the oil and gas industry*, Wiley-VCH, 2020, 464 pp.
7. E. Barmatov, J. Geddes, T. Hughes and M. Nagl, Research on corrosion inhibitors for acid stimulation, *NACE Corros.*, 2012, 1573.
8. A.A. Kruzhilin, D.S. Shevtsov, A.Y. Potapov, K.S. Shikhaliev, O.A. Kozaderov, Ch. Prabhakar and V.E. Kasatkin, Novel inhibitory compositions based on 4,5,6,7-tetrahydro-[1,2,4]triazolo[1,5-*a*]pyrimidin-7-ol derivatives for steel acid corrosion protection, *Int. J. Corros. Scale Inhib.*, 2022, **11**, no. 2, 774–795. doi: 10.17675/2305-6894-2022-11-2-22
9. D.V. Lyapun, A.A. Kruzhilin, D.S. Shevtsov, Y.V. Aseeva and K.S. Shikhaliev, Corrosion inhibition of steel by selected homologues of the class 3-alkyl-5-amino-1*H*-1,2,4-triazoles in acidic media, *Cond. Mat. Interph.*, 2022, **24**, no. 1. 59–68. doi: 10.17308/kcmf.2022.24/9056
10. A.A. Kruzhilin, D.V. Lyapun, D.S. Shevtsov, O.A. Kozaderov, A.Yu. Potapov, I.D. Zartsyn, Ch. Prabhakar and K.S. Shikhaliev, New [1,2,4]triazolo[1,5-*a*]pyrimidin-7-one corrosion inhibitors for copper in chloride environments, *Int. J. Corros. Scale Inhib.*, 2021, **10**, no. 4, 1474–1492. doi: 10.17675/2305-6894-2021-10-4-7
11. F. Mansfeld, Tafel slopes and corrosion rates obtained in the pre-Tafel region of polarization curves, *Corros. Sci.*, 2005, **47**, no. 12, 3178–3186. doi: 10.1016/j.corsci.2005.04.012
12. N.A. Negm, M.F. Zaki, M.M. Said and S.M. Morsy, Inhibitory action of biodegradable modified vanillin on the corrosion of carbon steel in 1 M HCl, *Corros. Sci.*, 2011, **53**, no. 12, 4233–4240. doi: 10.1016/j.corsci.2011.08.034
13. P. Lowmunkhong, D. Ungthararak and P. Sutthivaiyakit, Tryptamine as a corrosion inhibitor of mild steel in hydrochloric acid solution, *Corros. Sci.*, 2010, **52**, no. 1, 30–36. doi: 10.1016/j.corsci.2009.08.039
14. M. Oubaaqa, M. Ouakki, M. Rbaa, A.S. Abousalem, M. Maatallah, F. Benhiba and A. Zarrouk, Insight into the corrosion inhibition of new amino-acids as efficient inhibitors for mild steel in HCl solution: Experimental studies and theoretical calculations, *J. Mol. Liq.*, 2021, **334**, 116520. doi: 10.1016/j.molliq.2021.116520

♦ ♦ ♦